DOI : https://doi.org/10.7186/wg512202503

Effectiveness of sieving and grinding in measuring the concentration of rare earth elements from ion adsorption clay in Lumut, Perak

Kribagiry Thamilarasan*, Mohd Suhaili bin Ismail

Geosciences Department, Universiti Teknologi PETRONAS, 32610 Seri Iskandar, Perak, Malaysia
*Corresponding author email address: kriba.arasan96@gmail.com

Abstract: This study examines the effect of pre-treatment techniques of sieving and grinding on the concentration and extractable yield of rare earth elements (REEs) from ion adsorption clay (IAC) in Lumut, Perak. Three 3 kg samples were prepared: raw (untreated), sieved to <600 µm, and ground to <600 µm. The REE concentrations in the digested samples were analysed using Inductively Coupled Plasma Mass Spectrometry (ICP-MS), while the mineralogical composition was determined using X-ray Diffraction (XRD). The results showed that sieving significantly enriched light REEs (LREEs), with La and Nd up 38.7% and 40.1%, respectively, compared to the raw sample. However, only 1.65 kg of sample was retained post-sieving, resulting in a lower total recovery of La (76.3%). In contrast, grinding retained 2.92 kg and yielded a higher La recovery (84.5%) despite a lower concentration. These findings demonstrate a trade-off between concentration and mass yield: sieving is effective for enriching REEs in fine fractions, whereas grinding maximizes total extractable REEs. This study emphasizes the importance of integrating both concentration and mass balance in evaluating REE processing methods. It supports sieving as a selective enrichment technique and grinding as a superior alternative for maximizing total recovery from IAC.

Keywords: Ion adsorption clay, rare earth elements, sieving, grinding, minerals, Malaysia

INTRODUCTION

Rare earth elements (REEs) play a vital role in modern world technology today due to their distinctive properties, making them essential for various applications. There are 17 types of REEs, each having their own unique properties such as luminescence, magnetism, and catalytic capabilities (Haxel *et al*., 2002). REEs are utilised in various industries, including advanced manufacturing and electronics, serving as catalysts, additives, and essential components in specialized materials (Gschneidner *et al*., 2009). REEs are also essential components in magnets used in microphones, electric scooters, and motherboards. Additional examples of broader REEs application include smartphones, monitors, televisions and smartwatches. The relevance of REEs continues to grow as technology advances, making them impossible to be replaced, becoming an essential component of our contemporary world.

REEs are typically classified into two groups based on their atomic weights: light rare earth elements (LREE) and heavy rare earth elements (HREE) (N.S. Duzgoren-Aydin & Aydin, 2008). LREEs namely lanthanum (La), cerium (Ce), praseodymium (Pr), neodymium (Nd), promethium (Pm), and samarium (Sm) are more abundant and have a broader range of applications in electronics and metallurgic industries. Meanwhile, HREEs consist of europium (Eu), gadolinium (Gd), terbium (Tb), dysprosium (Dy), holmium (Ho), erbium (Er), thulium (Tm), ytterbium (Yb), and lutetium (Lu). It is normally less abundant but has more specific applications, such as magnet production for batteries. Understanding both HREE and LREE categories is essential for distinguishing the distinctive properties and applications of REEs. This can help to develop a successful and environmentally friendly technology.

Malaysia is poised to become a leading producer of REEs, with ion adsorption clay (IAC) deposits accounting for a substantial share of its resources. The IAC is primarily composed of clay minerals with the unique capacity to preferentially adsorb rare earth ions from

0126-5539; 2682-7549 / Published by the Geological Society of Malaysia.

water (Sanematsu *et al*., 2011). According to Sobri *et al*. (2023), IAC makes an extremely valuable REEs source, specifically LREEs. Weathered granite is closely related to IAC, and clay minerals found in IAC have a strong affinity for rare earth ions. Thus, IAC deposits are ideal for rare earth element extraction (Khairulanuar *et al*., 2022).

However, the development of effective physical mineral processing techniques prior to REE extraction remains a challenge. The extraction of LREE from IAC is also hampered by complex extraction techniques (Gkika *et al*., 2024) and high processing costs (Saskatchewan Research Council, 2015) are also challenges faced in. As a result, there is an urgent need for research into developing efficient and environmentally friendly techniques to process the IAC before extracting REEs from IAC deposits. Mineral processing is a critical step in many industrial processes, particularly those involving solid materials. It begins from treating the material in preparation for further operations like heat treatment and mechanical processes (Bamber *et al*., 2008). The most common pre-treatment techniques are sieving and grinding.

The particle size reduction process for solid material is known as the grinding method. The intended particle sizes and the specific properties of the material used dictate the grinding method used. Grinding processes can be classified into three types: which are crushing, ball milling and mortar grinding. Crushing is used to break down large chunks of material into smaller pieces. In contrast milling is utilized for finer particle sizes and is frequently associated with the use of balls or other grinding media. Grinding, on the other hand, is influenced by characteristics such as particle hardness, which requires a high energy level when working with harder materials. Particle size distribution has an impact on the grinding process as the initial size distribution of the material influences the grinding time and energy required (H. Du Plessis *et al*., 2007). Finally, the type and size of grinding media affects grinding efficiency and particle size distribution.

Sieving is the process of separating particles according to their size. It involves passing the material through a sieve or mesh with specific openings. Particles smaller than the openings pass through, while larger particles remain on the sieve. There are three types of sieving: mesh sieves, perforated plate sieves, and vibrating sieves. A mesh sieve employs wire mesh or woven fabric to sieve, whereas a perforated plate sieve uses holes in the plate. Vibrating sieves use wire mesh sieves that vibrate to improve separation efficiency, such as the ROTAP Sieve equipment used in most laboratories. The particle size distribution in the material impacts the efficiency of sieving, as does the size of the mesh, which plays a major role in sieving, as the larger the openings of the sieve, the faster the material can be sieved. Mesh size also determines the separation cut point in the material being sieved. Sieving techniques might also affect the sieving process. The method used to agitate the material on the sieve can influence the separation efficiency. Grinding and sieving are critical pre-treatment processes adopted by various industries, including mining, metallurgy, pharmaceuticals, and food processing. By reducing the particle size and separating materials based on size, grinding and sieving can improve the efficiency and product quality of subsequent processes (Justiniano *et al*., 2022).

Geological setting

The study area, which coincides with the IAC location, is in Lumut, in Manjung District, Perak (Figure 1). Manjung District is in the western region of Peninsular Malaysia. Even though Manjung is not directly positioned within the Bintang granite range, it is still geologically impacted by the granite intrusion. Granites in Peninsular Malaysia are classified into I-type in the Eastern Belt, S-Type in Central Belt and both I-type and S-Type in the Western Belt. According to Frost & Ronald Frost (2011), the granite in the study area is an S-type granite.

The formation of the IAC deposit in the study area is closely linked to the region's geological history. Over millions of years, weathering processes on the granite and granodiorite have released REEs into the environment (Middelburg *et al*., 1988). In the Manjung region, clay minerals in the granite adsorbed rare earth ions, resulting in the formation of IAC. The presence of major clay minerals such as kaolinite, illite, and montmorillonite, as observed in the Bintang range granite, is key to the geological characteristics of the IAC deposits in Lumut (Yaraghi *et al*., 2020). Lumut's IACs are recognized for having relatively high concentrations of REEs, particularly La, Pr, and Nd. The distinct geological conditions in Lumut have resulted in favourable environments for the formation of the IAC deposits. Consequently, this area has become an important source of REEs for Malaysia.

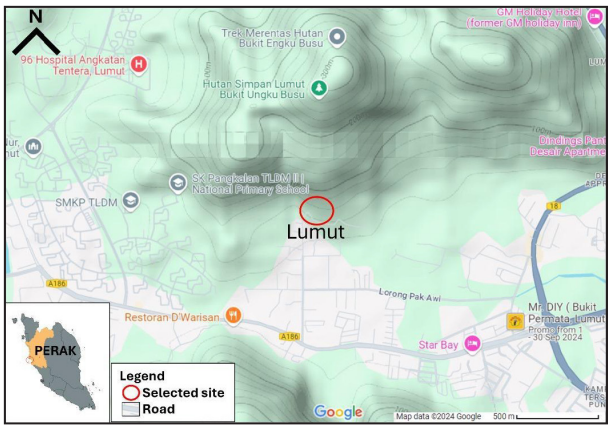

Figure 1: Map showing the location of the study area.

REEs deposits are generally classified based on their formation mechanism and mineralogical properties. Bünzli & Mcgill (2018) noted that the primary REEs deposits are the result of igneous and hydrothermal activity, whereas secondary deposits, mainly placer deposits and ion-adsorption clay deposits, are formed by weathering and sedimentary processes. Chemical weathering processes caused the REEs concentration within igneous weathering profiles, forming placer deposits (Fu *et al*., 2019). However, ion-adsorption clay deposits contain a higher concentration of REEs. Weathered granite crusts form in temperate and tropical climates as a result of numerous processes, such as metamictization and the presence of slightly acidic surface conditions that cause bedrock minerals to transform into secondary minerals such as clay minerals (White & Brantley, 2003). The metamictization process causes radioactive minerals to change texture from completely crystalline to fully metamictized forms (Meldrum *et al*., 1998).

Minerals containing REEs include high concentrations of radioactive elements, particularly uranium and thorium, which can cause host minerals such as micas and feldspars to partially erode in texture, increasing the likelihood that some rock-forming minerals will convert to clay minerals (Balan *et al*., 2001). Samples were collected along the "Lorong Mohd Nazir" road, on an exposed outcrop by the hillside. Surface sampling was conducted, of which about 1 meter of exposed outcrop depth was removed to collect approximately 10 kg of fresh soil sample.

METHODOLOGY

Sample collection and processing

The methodology adopted for this research mainly focused on the pre-treatment of the IAC. Approximately 9 kg of samples were collected from the study location in Lumut. The sample collected from the outcrop (Figure 2) was a whitish-beige coloured clay. Due to the moisture content, the grain size is generally fine, with small clumps of clay, while orange-coloured lines indicate the presence of iron oxide. Grinding and sieving are two common pre-treatment methods for preparing materials for further processing. The two techniques are crucial for reducing particle size, improving homogeneity, and removing impurities before they undergo the REEs extraction process (Khanuja & Dureja, 2021).

All the samples were air dried to avoid any additional changes in chemical properties that might result from heat drying. The samples were then coned and quartered to obtain a representative sample, which was subsequently divided into three equal portions weighing 3 kg each, as outlined in Figure 3. To ensure equal weight, the samples were weighed using a measuring balance. The first batch sample labelled Sample A was preserved as a raw sample to determine the REEs concentration and mineral composition without any pre-treatments. The results from Sample A were used as a theoretical reference value for comparing the other two samples. The second batch was sieved to -600 microns using a ROTAP Siever and designated Sample B, while the third batch was grinded to -600 micron with a mortar grinder and labelled as sample C. The ROTAP Siever and mortar grinder were obtained from the Geoscience Laboratory of University Technology Petronas (UTP). After pre-treatment, samples A, B, and C were sent for X-ray diffraction XRD and Inductively Coupled Plasma-Mass Spectrometry (ICP-MS) analysis to examine the mineral composition and determine the concentration of REEs in the samples, respectively. The XRD analysis was conducted by Orogenic Resources Sdn. Bhd. in Hulu Langat, Selangor, where they used the

Figure 2: On-site view of sampling point.

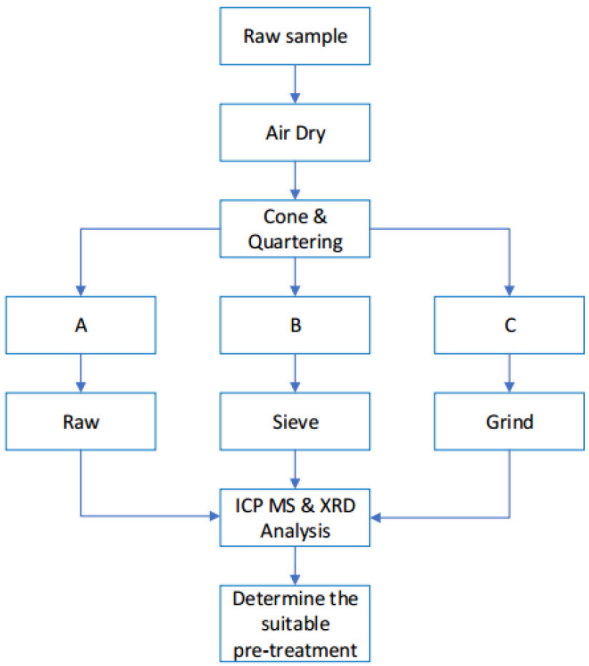

Figure 3: Methodology flowchart of the study.

PDXL software to interpret the XRD graph. Meanwhile, the ICP-MS analysis was conducted at the Rare Earth Element Analytical Laboratory at UTP.

Using the ICP-MS analysis results, the percentage of enrichment from Sample A was determined. The percentage of recovery was calculated using the formula below to determine the optimal pre-treatment method for REEs concentrated in the IAC:

Relative Enrichment % = (*Actual concentration*)/(*Theoretical concentration*) * 100% (1)

Whereby,

Actual concentration = The concentration of REEs from Grind or Sieve sample

Theoretical concentration = The concentration of REEs from Raw sample

Following the pre-treatment process, some samples from Sample B and Sample C were either lost or retained. Sample B retained 1.65 kg from the original 3 kg of the total sample processed, whereas Sample C retained 2.92 kg with the remaining 0.08 kg lost during the grinding process. The total mass of each element was then calculated followed by the actual percentage of recovery. The formulas are as below:

Element mass (*mg*) = *concentration* (*ppm*) * *retained sample mass* (*kg*)

Recovery % = (*Element mass in processed sample* (*Sample B or C*))/(*Element mass in Sample A*) * 100%

Geochemical analysis

• XRD analysis

The sample preparation for XRD analysis began by grinding the obtained sample in a pulveriser to an estimated 50-micron particle size. The sample was mounted onto a suitable sample holder, which is often in round shape. The surface was then flattened and smoothed for a uniform x-ray exposure. The sample was also pelletized, when necessary, before the start of the analysis. Though optional, pelletizing is typically used if the sample is unable to hold its shape and is scattering around.

XRD graphs looks way more complicated. XRD graphs comprise the X-axis representing the diffraction angle of X-rays, and the Y-axis representing the intensity (counts). Each peak corresponds to a set of planes within the crystal structure that satisfy Bragg's Law, indicating a specific crystal structure and lattice spacing. Bragg's Law relates the 2θ value at which a peak occurs to the spacing of the crystal planes, also known as d-spacing. The peak intensity reflects the number of crystal planes diffracting X-rays at that angle, indicating the degree of crystallinity and preferred orientation.

To interpret the graphs, the peaks were identified on the graph. The peaks were then assigned to crystal planes, by matching the peak positions which is the 2θ values with the corresponding crystal planes using reference ICSD databases. The peak intensities were quantified by measuring the height or area of each peak to determine the relative intensity of each reflection, followed by the PDXL software to quantify the minerals. Once the mineral was identified, all identified minerals were selected from the database and compared to the measured diffractogram to quantify the values using Rietveld refinement in the PDXL software. Lastly, the XRD analysis results were displayed in a table format. The untraced peaks were considered as total clay (undetectable in this process).

• ICP-MS analysis

There are several digestion methods, which are divided into two categories: open vessel digestion and closed vessel digestion. Open vessel digestion often employs a steam bath or hot stirrer., whereas manual digestion employs both a steam bath and hot plate stirrer, as well as hydrofluoric acid, sulphuric acid and hydrochloric acid. In the fusion diffusion method, x-ray flux, hydrogen peroxide with nitric acid or hydrochloric acid are used alongside a hot plate stirrer. Meanwhile for closed vessel digestion, a microwave system is used. There are two methods: pressurized autoclaves using nitrogen gas and nitric acid or using aqua regia, which does not require gas. This is dependent on the type of microwave machine used. Cross contamination and undissolved silica are two common challenges encountered throughout each stage. Silica only digest when using hydrofluoric acid but if there is no hydrofluoric acid present, filtration of the digested solution is carried out once it has competed the digestion.

In this study, Anton Paar's Microware Digestion System was employed for closed vessel digestion without external pressure using nitrogen gas in. About 200 mg of samples was weighed using a weighing scale and placed in the digestion vessel. The vessels were then placed in the fume hood and filled with 9 ml of nitric acid and 3 ml of hydrochloric acid. The vessels were sealed tightly and placed into the machine to digest using the EPA 3051A procedure. After digestion, the digested samples were filtered and transferred to a 100 ml volumetric flask, where ultrapure water was added up to the 100 ml line mark on the flask before being sent for ICP-MS analysis.

ICP-MS analysis is used to determine the concentration by elements. To reduce the contamination effect on the machine, dilution is required prior to starting the analysis. Digested solids samples were already diluted in the filtering and transfer process to the volumetric flask from the vessel. Meanwhile, liquid samples such as leachate, were diluted to x100 dilution in a 25 ml volumetric flask

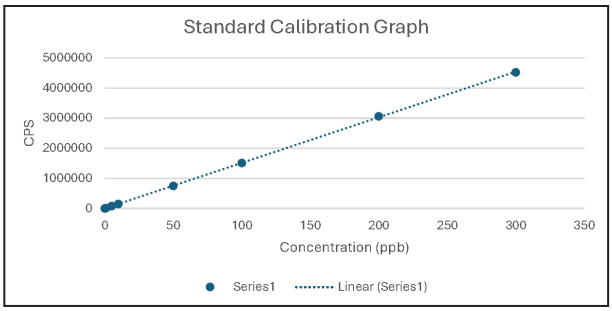

Figure 4: Standard calibration graph.

prior to analysis, and 2.5 ml of the liquid samples were pipetted into the flask, which was then filled with ultrapure water up to the indicated line. The flask was shaken to thoroughly mix the solution, transferred to a sample vial and lastly placed in the machine for the analysis.

The findings of the ICP-MS analysis are directly provided in table format. To cross-verify the results, the standard calibration graph was manually plotted for each element. Figure 4 depicts an example standard calibration graph of one of the elements analysed, plotted count per second (cps) against concentration (ppb). The cps of each element from each sample was compared in the graph and the cross-verification was carried out.

RESULTS AND DISCUSSION

XRD analysis

Table 1 shows the mineral composition of a sample analysed in three distinct states: Sample A, Sample B and Sample C, expressed as a weight percentage (%W). Table 1 summarises XRD results from APPENDIX A (i, ii, & iii) to enhance clarity and comprehension. The XRD data suggest that there are six types of minerals: quartz, plagioclase, K-feldspar, calcite, gibbsite, and total clay. Quartz, plagioclase, and K-feldspar are the most prevalent minerals in all three samples, indicating that the source rock material is composed of these minerals. Physical mineral processing has significantly altered the mineral composition, particularly in terms of quartz, plagioclase, and total clay weight percentages. Following the sieving process, the percentage of quartz decreased significantly, but the percentages of plagioclase, K-feldspar, and total clay increased, indicating that the sieving removed a portion of the quartz-rich material. There is also a slight decrease in the weight percentage of quartz and plagioclase in Sample C compared to Sample A. The weight percentages of minor minerals such as calcite and gibbsite vary slightly across different samples. To ensure accuracy, the total mineral composition of each sample was normalized to 100%, accounting for all detected phases. Overall, the grinding and sieving pre-treatment methods influenced the mineral composition; whereas the weight percentage of predominant minerals remained consistent with variations observed among the minor components. This XRD analysis is crucial for understanding the geological characteristics of the samples and assessing their potential applications.

Table 1: Summarized XRD results in weight percentage.

Bulk Mineralogy Composition (wt%)			
Sample / Mineral	Sample A	Sample B	Sample C
Quartz	37.2	22.3	36.1
Plagioclase	14.6	21.7	11.3
K-Feldspar	28.7	27.5	28.2
Calcite (Fe-Cal)	0.2	0.4	0.5
Gibbsite	3.8	4.2	3.1
Clay	15.5	23.9	20.8
Total	100.0	100.0	100.0

ICP MS analysis

The ICP MS analysis results for Samples A, B, and C from Appendix B are plotted in Figure 5. The x-axis lists the REEs, while the y-axis displays the concentrations of the elements in parts per million (ppm). Each element and its concentration are represented by individual bars on the graph. The samples mostly contain higher concentrations of various REEs, including La, Ce, Pr, Nd, and Y. The sieving and grinding processes influenced the overall REEs concentration, whereas a smaller particle size impacted the concentration of La and Ce, for example, resulting in an increase in their concentration following the process.

On the other hand, some REEs, such as Nd and Sm, have constant or decreased concentrations. Materials rich in rare earth elements are more likely to contain abundant LREEs than HREEs, which can be associated with the REEs distribution. La and Ce concentrations increased significantly, suggesting that they were potentially extracted during the leaching process. Several factors

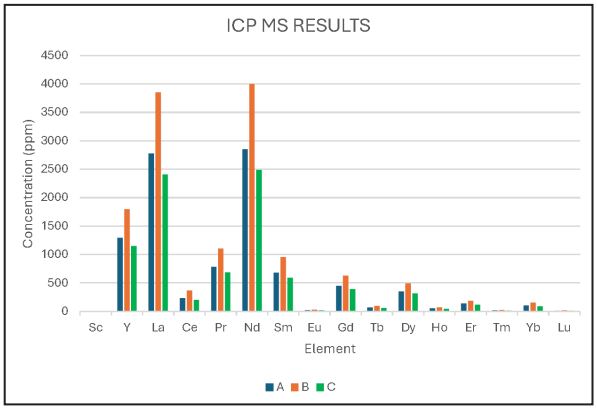

Figure 5: ICP-MS results for Samples A, B, and C.

such as particle size distribution, mineral liberation and removal of impurities, may have contributed to the higher concentration of REEs in Sample B compared to Samples A and C.

There are different particle size particle and sieving method to sorts the sample into the specific categories. The increased concentration for the sieved sample could be attributed to the REEs' association with a specific particle size. Furthermore, sieving can aid in the release of REEs from the associated REE-bearing minerals, greatly improving REEs extraction. This approach will be advantageous for releasing bonds between the REEs and REE-bearing minerals. Furthermore, by directing to a higher concentration of the elements in sample B, sieving can effectively remove impurities that may delay the analysis or the extraction of REEs.

Sample C has a lower REEs concentration than Samples A and B, most likely due to particle size reduction, alterations in mineral composition, and the loss of small particles in dust form. Grinding appears to have reduced the particle size and increased the surface area of exposure of the REE-bearing mineral, but has also produced a finer matrix, making REEs extraction more challenging. Furthermore, mechanical stress is exerted during the grinding process, altering the composition or structure of the minerals and affecting approachability of the REEs inside the mineral lattice. Another factor contributing to the decreased concentration of REEs in Sample C is the loss of sample, which may contain REEs, during the grinding process in the form of dust or fine particles.

Relative enrichment and true recovery

Relative enrichment

Relative enrichment can quantify the difference in REEs concentration (in ppm) after sieving and grinding, using the raw sample (Sample A) as a baseline. Figure 6 depicts the relative enrichment (%) of each element in the sieved sample (Sample B) and ground sample (Sample C), compared to the raw sample. Across all REEs, sieving (Sample B) produced higher relative enrichment compared to grinding (Sample C). Light REEs (LREEs) such as La, Ce, Pr, and Nd were significantly enriched in the sieved fraction, with La increasing by 38.7% and Nd increasing by 40.1% compared to the raw sample. This suggests that the <600 µm fine fraction remained after sieving the preferentially concentrated REE-bearing minerals, which can be attributed to the physical separation of REE-hosting clays from coarser quartz and feldspar. Conversely, the ground sample (Sample C) exhibited lower relative enrichment values, with La and Nd decreasing by 13.3% and 12.8%, respectively, relative to the raw sample. This suggests that grinding, while reducing particle size, may have homogenized the sample material without significantly enhancing REE concentration. Additionally, grinding may generate very fine dust particles that are either lost or difficult to fully digest, slightly diluting the apparent REE content. For heavy REEs (HREEs), both processing methods produced a more moderate effect, with enrichment levels varying between elements. In several cases, sieving slightly increased HREE concentration, but the overall trend indicates that LREEs benefitted the most from the sieving process.

Total recovery

Figure 7 compares the total recovery of REEs from the initial 3 kg of raw material for the sieved and ground samples, with retained weights of 1.65 kg and 2.92 kg, respectively. This combines both the REE concentration (ppm) and the actual mass retained after processing, providing a realistic estimate of extractable element mass for each approach. While sieving increased ppm concentrations in many REEs, this did not translate to higher total recoveries. For instance, although La concentration increased from 2779 ppm in the raw sample to 3853 ppm in the sieved sample, only 1.65 kg of material was preserved after sieving. The recovered La mass was 6.36 g, which accounts for just 76.3% of the original La amount present in the raw sample. In comparison, the ground sample (Sample C) retained nearly the full mass (2.92 kg), and despite having a lower La concentration (2411 ppm), it yielded 7.04 g of La, or 84.5% recovery, which is closer to the original raw sample yield of 8.34

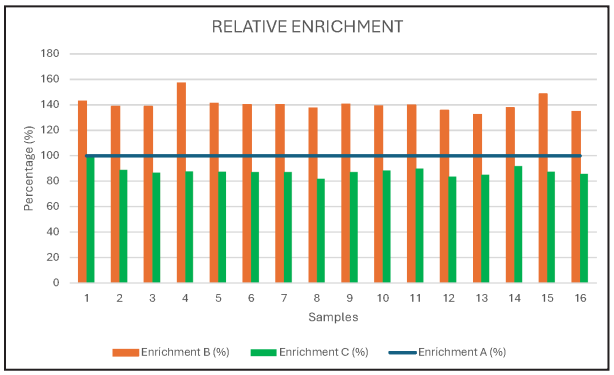

Figure 6: Relative enrichment percentage graph.

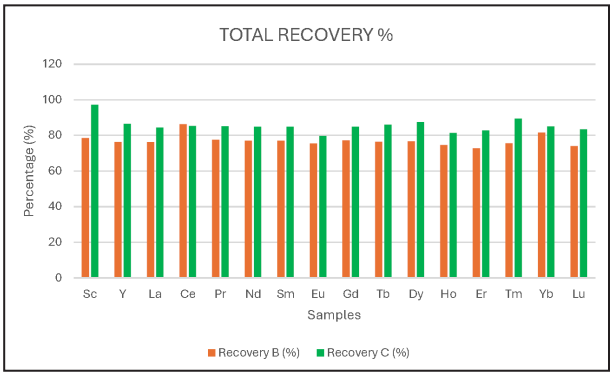

Figure 7: Total recovery percentage graph.

grammes. The element mass can be referred in APPENDIX D. This trend is consistent across most REEs: grinding recovers more total REE mass, while sieving enriches REEs in the retained fine fraction but discards coarse material that still contains recoverable REEs. These findings underscore the importance of mass balance when evaluating processing techniques. High concentration does not imply high recovery, and any preprocessing methods that discards part of the sample (e.g., sieving) must be evaluated for its overall impact on extractable yield.

Interpretation

The comparative analysis of REEs concentration and mass recovery across the raw (Sample A), sieved (Sample B), and ground (Sample C) samples reveals vital insights into the effectiveness of pre-treatment methods for processing IAC. A better understanding of processing efficiency is obtained by examining both relative enrichment (concentration difference) and total REE recovery (mass yield from original sample). The sieved sample (Sample B) exhibited a significant increase in REE concentration (ppm) relative to the raw sample, particularly for LREEs such as La, Ce, Pr, and Nd. For example, the La concentration increased from 2779 ppm in the raw sample to 3853 ppm in the sieved sample, representing an enrichment of approximately 138.7%. This suggests that sieving effectively concentrated REE-bearing clay particles in the <600 μm fraction while removing non-REE-bearing coarse material (e.g., quartz, feldspar). In contrast, ground samples (Sample C) revealed either minor enrichment or slight dilution of REE concentrations when compared to the raw sample, implying that homogenization alone is less effective in concentrating REEs within the sample matrix. Despite higher concentrations, the sieved sample retained only 1.65 kg of the original 3 kg mass, resulting in a reduced total REE recovery. Only 6.36 g of La was recovered, compared to 8.34 g in the raw sample, for a recovery rate of 76.3%. In comparison, the ground sample retained 2.92 kg of material and recovered 7.04 g of La (84.5% recovery), demonstrating that grinding, while less efficient at concentrating REEs, preserved more of the sample and therefore had a higher overall extraction potential.

CONCLUSION

This study provides a detailed evaluation of the mineral composition, REE potential, and pre-treatment effectiveness in processing ion adsorption clay (IAC) from Lumut. The analysis revealed a strong correlation between mineral assemblage and REE concentration, with plagioclase and gibbsite identified as key REE-hosting minerals (Li & Zhou, 2020). The ICP-MS results demonstrated that sieving increased the concentration of light REEs, with La and Nd enriched by 38.7% and 40.1%, respectively. However, this occurred at the expense of mass loss, as only 1.65 kg of material was retained, resulting in a lower total recovery of La (76.3%) compared to the raw sample. In contrast, grinding retained 2.92 kg of sample while achieving a higher total recovery of La (84.5%), despite its lower concentration. These findings highlight a trade-off between enrichment and recovery: sieving improves REE concentration for selective extraction, while grinding maximizes overall yield. The choice of method should align with the intended processing objective. Overall, this research underscores the significance of addressing both concentration and mass balance when evaluating pre-treatment strategies. Optimized processing, tailored to the mineralogical context of the deposit, can significantly enhance REE extraction efficiency from IAC.

ACKNOWLEDGEMENT

We thank Orogenic Resources Sdn. Bhd. for undertaking a thorough geochemical analysis. The authors would like to acknowledge the work of various people in the Geoscience Department at University Technology PETRONAS for their guidance and assistance in using the equipment to process the samples. We personally thank Dr Ismail bin Ibrahim (JMG Malaysia) for his assistance in the overall research conceptualization. Also, thank you to all my reviewers and editors for making this manuscript more valuable. The corrections and suggestions provided by anonymous reviewers and editors are highly acknowledged.

AUTHORS CONTRIBUTION

T.K. - paper conceptualization, literature review, sample processing, data compilation, analysis and interpretation, figure drafting, writing and editing; M.S.B.I. - interpretation, review, writing and editing.

CONFLICT OF INTEREST

The authors declare that there is no conflict of interest in connection with this article.

REFERENCE

Balan, E., Neuville, D.R., Trocellier, P., Fritsch, E., Muller, J.-P., & Calas, G., 2001. Metamictization and chemical durability of detrital zircon. American Mineralogist, 86(9), 1025–1033.

Bamber, A.S., Klein, B., Pakalnis, R.C., & Scoble, M.J., 2008. Integrated mining, processing and waste disposal systems for reduced energy and operating costs at Xstrata Nickel's Sudbury Operations. Mining Technology, 117(3), 142–153.

Bünzli, J.G., & Mcgill, I., 2018. Rare Earth Elements. Ullmann's Encyclopedia of Industrial Chemistry, 1–53.

Frost, C.D., & Ronald Frost, B., 2011. On Ferroan (A-type) Granitoids: their Compositional Variability and Modes of Origin. Journal of Petrology, 52(1), 39–53.

Fu, W., Luo, P., Hu, Z., Feng, Y., Liu, L., Yang, J., Feng, M., Yu, H., & Zhou, Y., 2019. Enrichment of ion-exchangeable rare earth elements by felsic volcanic rock weathering in South China: Genetic mechanism and formation preference. Ore Geology Reviews, 114, 103120–103120.

Gkika, D.A., Michail Chalaris, & Kyzas, G.Z., 2024. Review of Methods for Obtaining Rare Earth Elements from Recycling and Their Impact on the Environment and Human Health. Processes, 12(6), 1235–1235.

Gschneidner, K.A., Eyring, L., Lander, G.H., Bünzli, J.G., & Pecharsky, V.K., 2009. Handbook on the Physics and Chemistry of Rare Earths, Vol. 39. Elsevier, Amsterdam, North-Holland. 112 p.

H. Du Plessis, Kearsley, E.P., & H. Matjie, 2007. Effect of grinding time on the particle size distribution of gasification ash and Portland cement clinker. Joernaal van Die Suid-Afrikaanse Instituut van Siviele Ingenieurswese, 50(2), 18–18.

Haxel, G.B., Hedrick, J.B., Orris, G.J., Stauffer, P.H., & Hendley, J.W., 2002. Rare earth elements: Critical resources for high technology (Fact Sheet 087–02). U.S. Geological Survey. https://doi.org/10.3133/fs08702.

Justiniano, N.K., Velásquez, M.L., Zenteno, F G., & Rojas, M.L., 2022. Effect of Grinding and Sieving on the Coffee Properties: A Systematic Review. Proceedings of the 20th LACCEI International Multi-Conference for Engineering, Education and Technology: "Education, Research and Leadership in Post-Pandemic Engineering: Resilient, Inclusive and Sustainable Actions." July, 2022.

Khairulanuar, K.A., Segeran, L., Jabit, N., Ismail, S., Ibrahim, I., & Ariffin, K.S., 2022. Characterisation of rare earth elements from Malaysian ion-adsorption clay. Materials Today: Proceedings, 66, 3049–3052.

Khanuja, H.K., & Dureja, H., 2021. Recent Patents and Potential Applications of Homogenisation Techniques in Drug Delivery Systems. Recent Patents on Nanotechnology, 15.

Li, M.Y.H., & Zhou, M.-F., 2020. The role of clay minerals in formation of the regolith-hosted heavy rare earth element deposits. American Mineralogist, 105(1), 92–108.

Meldrum, A., Boatner, L. A., Weber, W. J., & Ewing, R.C., 1998. Radiation damage in zircon and monazite. Geochimica et Cosmochimica Acta, 62(14), 2509–2520.

Middelburg, J.J., van der Weijden, C.H., & Woittiez, J.R.W., 1988. Chemical processes affecting the mobility of major, minor and trace elements during weathering of granitic rocks. Chemical Geology, 68(3-4), 253–273.

N.S. Duzgoren-Aydin, & Aydin, A., 2008. Distribution of rare earth elements and oxyhydroxide phases within a weathered felsic igneous profile in Hong Kong. Journal of Asian Earth Sciences, 34(1), 1–9.

Sanematsu, K., Kon, Y., Imai, A., Watanabe, K., & Watanabe, Y., 2011. Geochemical and mineralogical characteristics of ion-adsorption type REE mineralization in Phuket, Thailand. Mineralium Deposita, 48(4), 437–451.

Saskatchewan Research Council, 2015. Can Innovation in Rare Earths Solve Processing Challenges? (26 January 2015). Src.sk.ca. https://www.src.sk.ca/blog/can-innovation-rare-earths-solve-processing-challenges. Accessed on 8th March 2025.

Sobri, N.A., Yunus, M.Y.B.M., & Harun, N., 2023. A review of ion adsorption clay as a high potential source of rare earth minerals in Malaysia. Materials Today: Proceedings, 2023.

White, A.F., & Brantley, S.L., 2003. Chemical weathering of silicate minerals. Reviews in Mineralogy and Geochemistry, 50(1), 1-22.

Yaraghi, A., Kamar Shah Ariffin, & Norlia Baharun, 2020. Comparison of characteristics and geochemical behaviors of REEs in two weathered granitic profiles generated from metamictized bedrocks in Western Peninsular Malaysia. Journal of Asian Earth Sciences, 199, 104385–104385.

APPENDIX A (i): Raw sample XRD Data

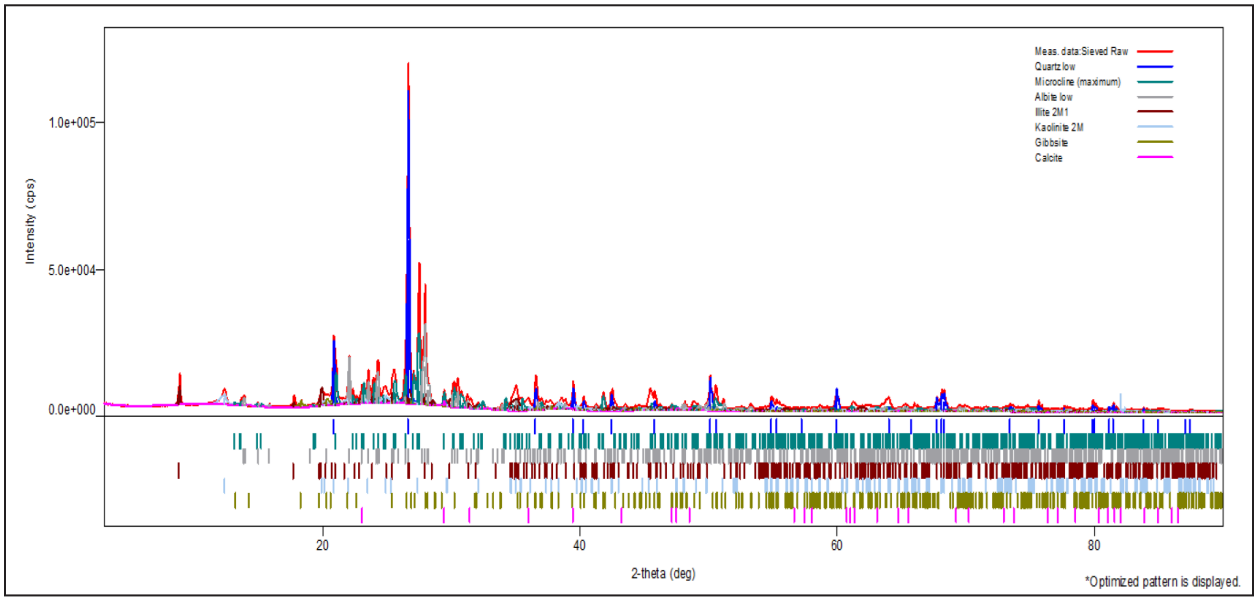

APPENDIX A (ii): Grind sample XRD Data

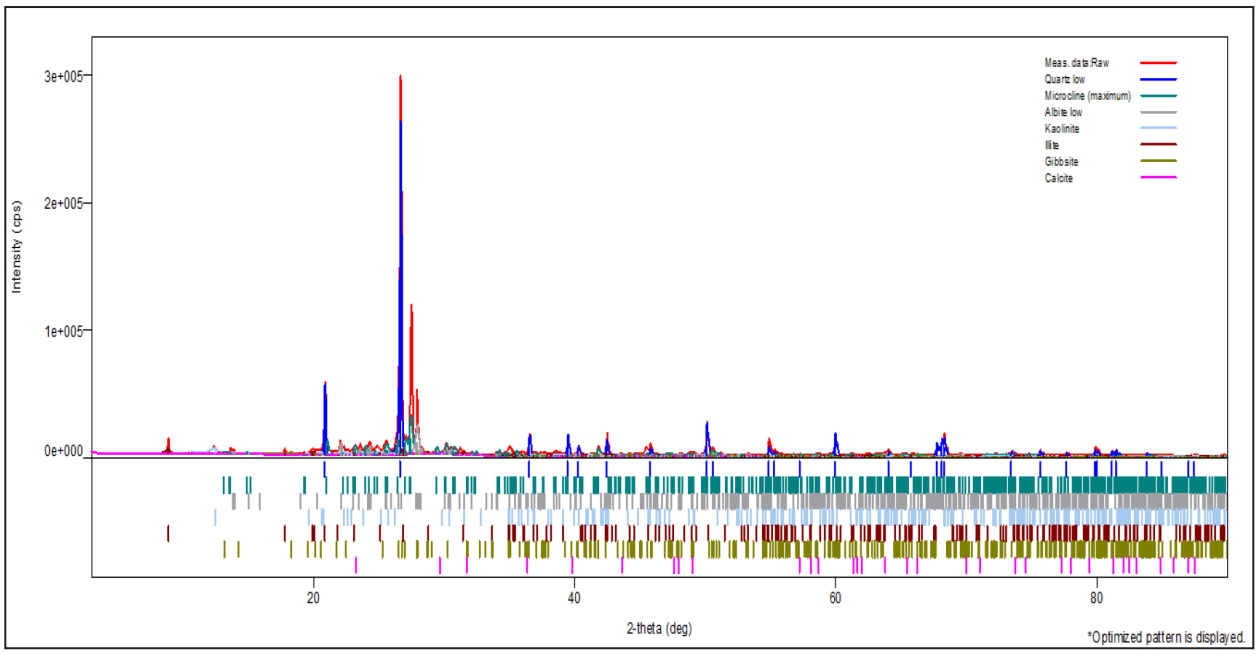

APPENDIX A (iii): Sieve sample XRD Data

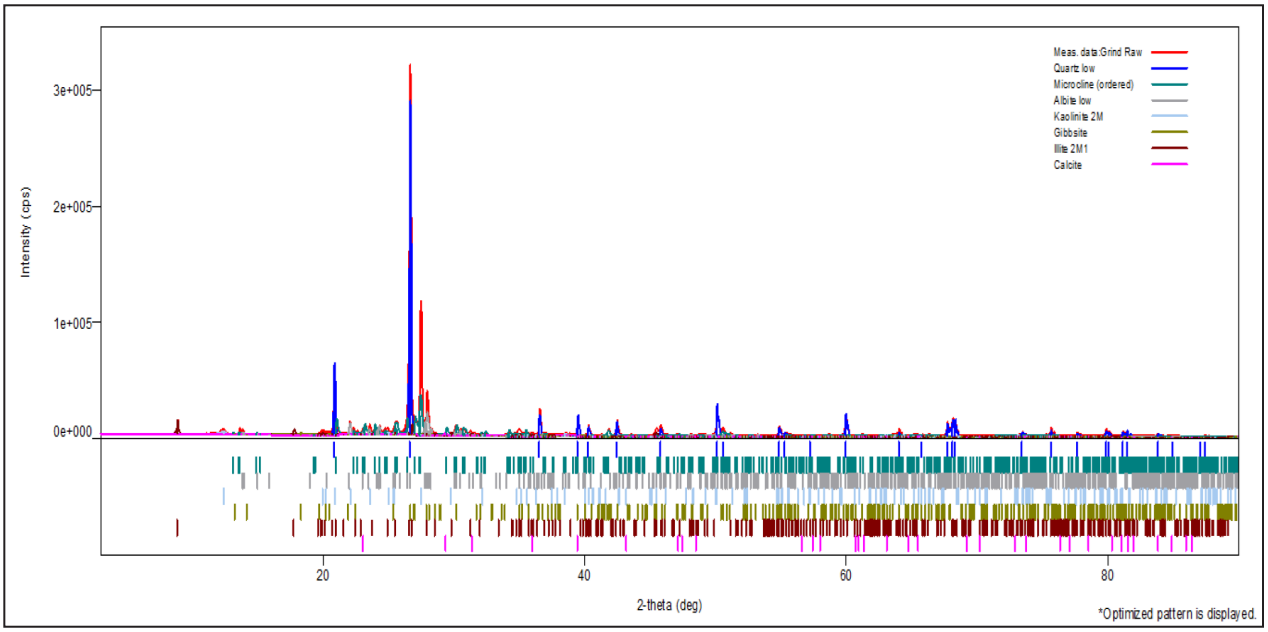

APPENDIX B: ICP MS concentration table in PPM unit.

Sample Name	SAMPLE A	SAMPLE B	SAMPLE C
Sc	1.0	1.4	1.0
Y	1295.4	1799.2	1152.0
La	2778.6	3853.1	2410.5
Ce	233.7	366.8	205.1
Pr	784.1	1107.6	686.4
Nd	2854.0	4000.0	2489.3
Sm	680.0	953.4	593.6
Eu	22.3	30.6	18.3
Gd	448.9	630.3	391.7
Tb	69.8	97.0	61.7
Dy	352.9	493.0	317.4
Ho	54.2	73.6	45.4
Er	140.1	185.5	119.2
Tm	17.8	24.5	16.3
Yb	105.2	156.1	92.0
Lu	13.0	17.5	11.1

APPENDIX C: Relative Enrichment

Sample Name	Enrichment B (%)	Enrichment C (%)
Sc	143.0	100.0
Y	138.9	88.9
La	138.7	86.8
Ce	157.0	87.7
Pr	141.3	87.5
Nd	140.2	87.2
Sm	140.2	87.3
Eu	137.3	81.9
Gd	140.4	87.3
Tb	139.0	88.5
Dy	139.7	89.9
Ho	135.7	83.7
Er	132.4	85.1
Tm	137.6	92.0
Yb	148.4	87.5
Lu	134.7	85.8

APPENDIX D: Element Mass

Sample Name	Total A (mg)	Total B (mg)	Total C (mg)
Sc	3.0	2.4	2.9
Y	3886.3	2968.6	3363.8
La	8335.9	6357.6	7038.7
Ce	701.2	605.3	598.8
Pr	2352.2	1827.5	2004.3
Nd	8562.1	6600.1	7268.7
Sm	2040.0	1573.1	1733.2
Eu	67.0	50.6	53.4
Gd	1346.6	1040.0	1143.9
Tb	209.3	160.0	180.3
Dy	1058.8	813.4	926.9
Ho	162.6	121.4	132.5
Er	420.4	306.1	348.2
Tm	53.3	40.3	47.7
Yb	315.6	257.6	268.7
Lu	38.9	28.9	32.5

APPENDIX E: Total Recovery

Sample Name	Recovery B (%)	Recovery C (%)
Sc	78.7	97.3
Y	76.4	86.6
La	76.3	84.4
Ce	86.3	85.4
Pr	77.7	85.2
Nd	77.1	84.9
Sm	77.1	85.0
Eu	75.5	79.7
Gd	77.2	84.9
Tb	76.5	86.1
Dy	76.8	87.5
Ho	74.6	81.5
Er	72.8	82.8
Tm	75.7	89.5
Yb	81.6	85.1
Lu	74.1	83.5

Manuscript received 8 January 2025;
Received in revised form 9 March 2025;
Accepted 8 August 2025
Available online 30 August 2025